Surface Morphology Diagram for Cylinder-Forming Block Copolymer Thin Films

Xiaohua Zhang,[†] Brian C. Berry,[†] Kevin G. Yager,[†] Sangcheol Kim,[†] Ronald L. Jones,[†] Sushil Satija,[‡] Deanna L. Pickel,[§] Jack F. Douglas,[†,*] and Alamgir Karim[†,*]

[†]Polymers Division and [‡]NIST Center for Neutron Research, National Institute of Standards and Technology (NIST), Gaithersburg, Maryland 20899, and [§]Center for Nanophase Materials Sciences, Oak Ridge National Laboratory, Oak Ridge, Tennessee 37831

ABSTRACT We investigate the effect of the ordering temperature (T) and film thickness (h_f) on the surface morphology of flow-coated block copolymer (BCP) films of asymmetric poly(styrene-block-methyl methacrylate). Morphology transitions observed on the ordered film surface by atomic force microscopy (AFM) are associated with a perpendicular to a parallel cylinder BCP microphase orientation transition with respect to the substrate with increasing h_f. "Hybrid" surface patterns for intermediate h_f between these limiting morphologies are correspondingly interpreted by a coexistence of these two BCP microphase orientations so that two "transitional" h_f exist for each T. This explanation of our surface patterns is supported by both neutron reflectivity and rotational SANS measurements. The transitional h_f values as a function of T define upper and lower surface morphology transition lines, $h_{fu}(T)$ and $h_{fl}(T)$, respectively, and a surface morphology diagram that should be useful in materials fabrication. Surprisingly, the BCP film surface morphology depends on the method of film formation (flow-coated versus spun-cast films) so that nonequilibrium effects are evidently operative. This morphological variability is attributed primarily to the trapping of residual solvent (toluene) within the film (quantified by neutron reflectivity) due to film vitrification while drying. This effect has significant implications for controlling film structure in nanomanufacturing applications based on BCP templates.

KEYWORDS: block copolymer films · surface morphology diagram · residual solvent

Block copolymers (BCP) involve the chemical linking of two or more polymer chains of different chemical species and these molecules self-assemble into complex supramolecular structures of interest in many applications. As with many polymer mixtures, there is a natural tendency of the polymer blocks to phase separate because of the relatively low entropy of mixing of polymer molecules, but chain connectivity frustrates macroscopic phase separation. Instead, the BCP components segregate at the molecular scale to express their thermodynamic antipathy.[1] In block copolymers composed of flexible polymer chain components, the constraints of packing and interfacial continuity produce the familiar morphologies of these materials in bulk: lamellae, gyroid, cylinders, or spheres depending on the volume fraction of the components.[1] Even more exotic nanoscale morphologies are formed in small amphiphilic molecules where dipolar and charge interactions are often also involved, but the self-organization of these structures has a similar microphase separation origin.[1] The interplay between bulk and interfacial energies that govern the ordering of BCP materials is modified when such films are confined to molecularly thin films where the interfacial energies of the solid substrate and the air interface contribute appreciably to the free energy of the ordered structures that form under film confinement.[2] Polymer films also tend to exhibit especially slow kinetics in their ordering and these effects are prevalent in affecting the properties of solution cast films of high molecular mass glass-forming polymers.[3] The ordering of block copolymers in thin films can then be expected to lead to a much richer range of morphologies than bulk materials because of both thermodynamic and kinetic factors and the potential opportunity to tune these morphologies by varying film thickness and substrate interaction. This situation also requires a greater understanding of the physics governing these changes in organization and the variables that control them. In particular, the control of microdomain ordering in BCPs is essential for utilizing these materials as lithographic templates and other applications in nanotechnology.[4,5]

It is generally appreciated from numerous previous theoretical and neutron scattering studies of block copolymer materials that a solid substrate can create an effective "field" that can perturb the BCP ordering over an appreciable distance and that this perturbation is related to the selective block copolymer interaction with the substrate and the strength of the interaction between
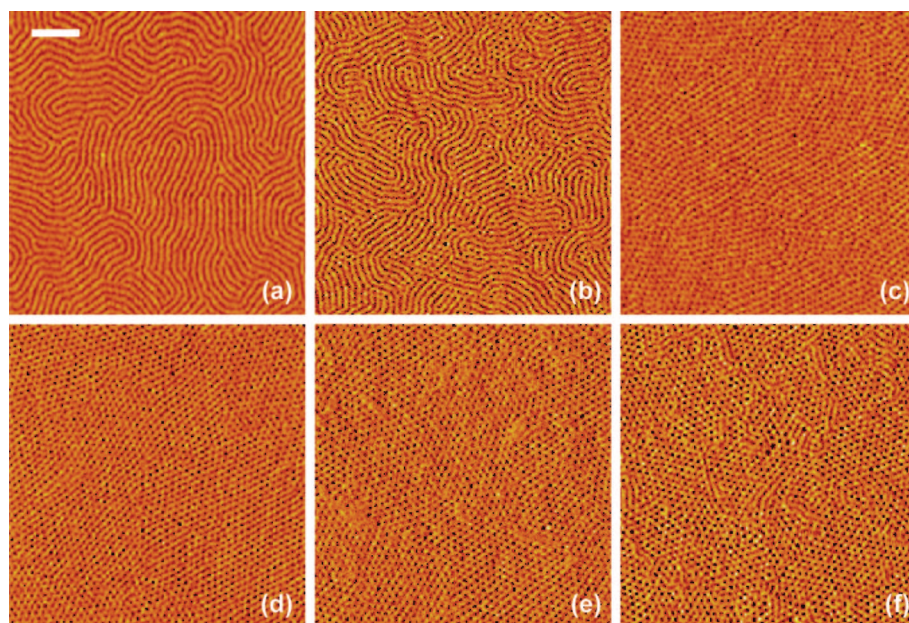
Figure 1. AFM phase images of flow-coated PS-*b*-PMMA block copolymers with different film thickness after annealing at 147 °C for 15 h: (a) 58, (b) 71, (c) 86, (d) 104, (e) 130, and (f) 168 nm. The scale bar in panel a corresponds to 200 nm and is applied to panels b−f.

RESULTS

Influence of Film Thickness and Annealing Temperature on BCP Film Surface Morphology. First, we give an overview of our morphological observations on flow-coated and ordered BCP films and our interpretation of these patterns, which we support below with neutron scattering measurements. Representative AFM phase images of PS-*b*-PMMA block copolymers with different film thickness h_f after ordering the sample at an annealing temperature of 147 °C for 15 h are shown in Figure 1. The PMMA component of PS-*b*-PMMA copolymer preferentially segregates to the plasma-treated silicon wafer substrate[1,13] (PMMA favors the silicon oxide substrate because of its lower wetting energy[14−16]). In Figure 1a, we observe the formation of cylinders that are oriented parallel to the substrate, which is natural given the strong segregation BCP conditions of the thin block copolymer film and the wetting characteristics of the solid substrate. For thicker films (Figure 1b), however, we find a "hybrid" morphology, consisting of cylinders oriented both parallel and perpendicular to the underlying substrate, where the fraction of cylinders oriented perpendicularly progressively increases with increasing film thickness, h_f. The surface patterns of still thicker films ($h_f > 86$ nm) correspond to cylinders oriented perpendicularly to the polymer interface, an orientation that does not match the orientation induced by the solid substrate (Figure 1c−f). Notably, this perpendicular cylinder morphology remains stable after a reasonably long annealing time of 87 h. An understanding of these morphological transitions requires a detailed study of the dependence of the surface patterns on h_f and T.

There is an additional "monolayer" film thickness regime in which h_f is comparable with characteristic BCP ordering dimension (determined below) L_0, where the cylinders evidently orient normal to substrate. Ham and co-workers[17] have recently studied this high confinement regime, but we expect new physical effects to arise in this regime due to a combination of residual solvent effects (see next section) and finite size perturbations of the BCP ordering. We thus avoid this "monomolecular" film regime in the present study.

Residual Solvent Effect in Cast Polymer Films. Nonequilibrium effects are often obvious in the formation of polymer films because of the general tendency of polymers to form glasses. In the present context, this phenomenon is demonstrated by simply altering the

the blocks themselves.[6] The effects of these substrate interactions on the surface morphology of BCP films supported on a solid substrate are not well understood, although there has been much progress recently in understanding surface pattern formation in lamellar forming BCP.[7] The roles of the casting solvent[8] and the physics of glass-formation[9] on the ordering of these films are also not well understood.

The influence of film confinement on the surface pattern formation in BCP films is attracting increasing attention because of the importance of this phenomenon in applications where these materials are being considered as nanoscale templates for various nanotechnology fabrication applications. For example, Suh *et al*.[10] predicted a transformation between perpendicular and parallel morphologies in cylindrical block copolymer domains when the difference in the surface tension between two polymer components of the block is sufficiently small and where the film thickness is less than a few repeat spacings. Krausch *et al*.[11] have actually observed such transitions in recent studies. Clearly a strong effect of film confinement on the BCP morphology exists, which depends on many parameters (*T*, polymer substrate interaction, block copolymer topology, *etc*.). In the present work, we perform a systematic study of the ordering of polystyrene-polymethyl methacrylate (PS-*b*-PMMA) block copolymer films that form cylinders in the bulk, a material of interest from an applications standpoint.[12] We are particularly interested in establishing the thickness h_f and T dependence and the prevalence of nonequilibrium effects on the surface morphology of these model block copolymer films, since these factors are relevant to fabrication efforts using these promising materials.

method of preparing the films, where the substrate, solvent, and BCP are unchanged. Figure 2 panels a and b contrast the morphologies of BCP films (annealed in a vacuum oven within a few hours after preparation, at 173 °C for 15 h) prepared by flow coating and spin coating, starting from the same casting solution where the films have essentially the same thickness. The surface patterns obtained by these casting methods are evidently qualita-

Figure 2. AFM phase images of PS-*b*-PMMA block copolymers with the same film thickness ($h_f \approx$ 154 nm) after annealing for 15 h at 173 °C. (a) Flow-coated film, (b) Spin-coated film and (c) Flow-coated film annealed at 50 °C for 3 d to remove residual solvent prior to high *T* annealing. The scale bar in panel a corresponds to 200 nm and also applies to panels b and c.

tively different. Notably, both flow-coating and spin-casting methods lead to highly reproducible results, despite the different surface patterns apparent in Figure 2. The film thickness in this comparison was chosen to specifically compare to our previous study of zone refinement on BCP films,[18] where the films were prepared by spin casting rather than flow coating. This former study also included control measurements that were not subjected to zone refinement and the observed pattern formation in this study is consistent with the image in Figure 2b.

The trapping of residual solvent in cast films due to the vitrification of the evaporating film is a recurrent problem in describing the phase behavior of thin polymer films. Understandably, this is a topic that few researchers want to discuss since solvent "impurities" can give rise to large effects relating to change in the polymer−substrate interaction and polymer−polymer interaction in both blends and block copolymer films. There has been previous work emphasizing the effect of the solvent evaporation process on BCP, rather than residual solvent in the already cast film on ordering when the temperature is raised above the glass transition at a later stage of BCP film processing.[8,19] In addition to modifying the thermodynamics of the film during film ordering, the presence of residual solvent within the cast film can also be expected to influence the dynamical heterogeneity of glass-formation, and thus indirectly influence the nonequilibrium morphology of the ordered BCP film (see discussion below).[9] We next utilize neutron reflectivity to establish the amount of residual solvent retained in our BCP films.

The high degree of contrast (the scattering length densities of PS-*b*-PMMA and deuterated toluene are 1.3×10^{-6} and 5.7×10^{-6} Å^{-2}, respectively) makes this an ideal technique for measuring even a small amount of residual solvent in flow-coated and spin-coated block copolymer films. Figure 3 shows neutron reflectivity (NR) observations on the *same* block copolymer, but with the film casting solvent replaced by its deuterated analogue for contrast purposes. The solid
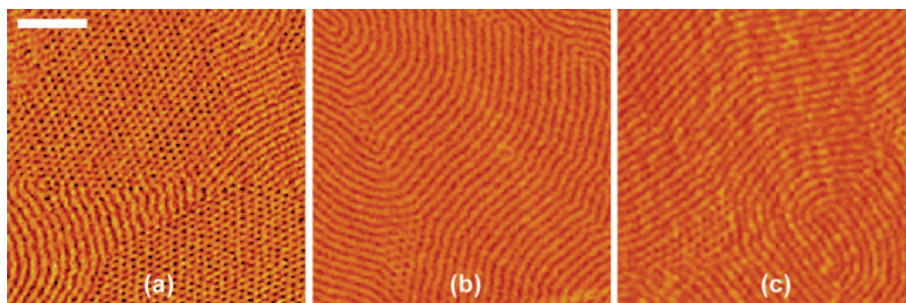
lines in this figure are best fits to our composition profile model and the resulting deuterated solvent composition profiles for spin-cast and flow-coated films are shown as insets to Figure 3a,b. (Detailed information about NR method and our fitting procedure are given elsewhere.[20]) The volume fraction profiles in this figure assume the hPS and hPMMA blocks have sufficiently similar scattering length densities so that we only distinguish solvent *versus* average polymer profile distribution, but not the details of the components of the block copolymer within the solvated film to which the NR is relatively insensitive. We rely upon the dPS-hPMMA system to extract information about the latter, as described later in the paper. The average polymer approximation is especially valuable in estimating the *total* toluene concentration in the film. In particular, we find unequivocally for both the spin-cast and flow-coated films that there is an appreciable amount of residual solvent ϕ_r left in the film after casting, $\phi_r = 12\%$ and $\phi_r = 16\%$, respectively, where here and below the toluene concentration ϕ_r units are volume %. The larger amount of residual solvent in the flow-coated films is probably a general phenomenon arising from a diminished convective flow in more slowly evaporating flow-coated films, which allows more solvent to become trapped near the solid film substrate at the point of vitrification while evaporating. The wedge-like shape of the solvent density profiles in Figure 3a,b indicates a general tendency for the solvent to accumulate near
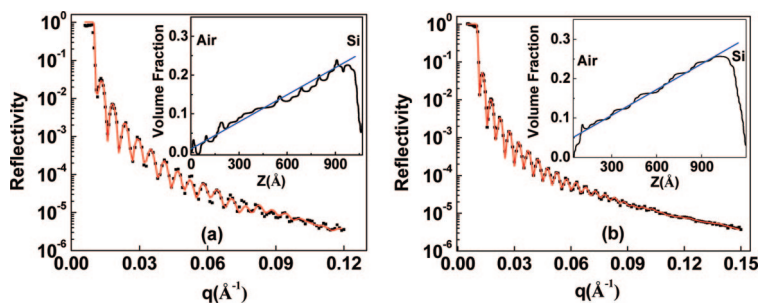

Figure 3. Neutron reflectivity measurements on PS-*b*-PMMA films cast with deuterated toluene. Panels a and b contrast spin-coated and flow-coated films, respectively, and the insets to these panels show the corresponding fitted deuterated toluene composition (volume fraction) profiles.

the solid substrate, and the observed concentration profile shape accords qualitatively with a recent molecular dynamics simulation of evaporating polymer films.[21] We also observe in Figure 3a that extrapolating the approximately linear toluene concentration gradient (fitted line in figure) to the polymer–air interface in the spin-coated film indicates a low concentration of solvent near the polymer–air boundary, $\phi_r \approx 1\%$, while the solvent composition in the flow-coated film gradient (fitted line in figure) extrapolates to a relatively high concentration at this boundary, that is, $\phi_r \approx 5\%$. Clearly, the presence of such a large amount of solvent at the free boundary in the flow-coated film should have a large impact on the interfacial energy of the film, which in turn should affect the film morphology. Thus, it is understandable that spun-cast and flow-coated films exhibit a different surface pattern formation.

Subjecting the film to thermal annealing, as described above, removes much of the residual solvent and our NR measurements indicate that the total volume fraction of residual solvent after thermal annealing at 93 °C for 7 h is $\phi_r = 2.6\%$. Note that there is no convenient way to anneal glassy BCP such as our films to remove the solvent without initiating the BCP ordering so that solvent effects on the ordered morphology are difficult to avoid in practice.

Initially, we were puzzled by the large amount of residual solvent indicated by our NR measurements, but then we were reassured to find that this phenomenon is consistent with previous studies of solvent cast films.[22,23] After the film is initially cast, the solvent evaporates rapidly and correspondingly the glass transition temperature T_g increases until the film vitrifies. If this is exactly true, then a measurement of the film T_g should allow a determination of the solvent composition from the known shift of T_g with solvent composition.[22,23] Specifically, PS films cast from toluene solutions at room temperature were found to have an appreciable residual toluene concentration, $\phi_r = 17.6 \pm 1.4\%$, the uncertainty being associated with the film T_g measurements.[22,23] Moreover, a correlation between the amount of residual toluene in cast PS films and the casting temperature[22,23] indicates that a film annealed at 93 °C should have a residual toluene concentration of about $\phi_r = 1.5\%$. Both of these toluene concentration estimates for macroscopic cast polymer films are in line with our NR observations. It is apparently *normal* for large quantities of residual solvent to be trapped in glassy polymer films and it is possible to tune this concentration at will by adjusting the casting temperature. For ultrathin films ($h_f \leq 200$ nm), there is even a greater enhancement for residual solvent to remain in PS films cast from toluene, even after annealing for long times above T_g,[24] an effect that can apparently influence the adhesion of BCP films to their substrate.[24] The even greater solvent retention in ultrathin films can be attributed to the combined effects of an attractive interaction of the solvent with the substrate[24] and a diminished solvent mobility in ultrathin films,[25] which can slow the rate of solvent evaporation.

There are positive consequences of this ubiquitous residual solvent effect. Our flow-coated films show a much higher propensity to form cylinders having a perpendicular orientation, an effect of great practical consequence if some means is used to stabilize the pattern formation. To gain insight into the residual solvent effect in our flow-coated films, we subjected the film shown in Figure 2a to a heat treatment in which the films were heated in an oven at 50 °C below T_g for 3 d to facilitate removal of the residual solvent from the film, and we subsequently let the BCP film order by annealing the film at 173 °C. The resulting surface pattern (Figure 2c) now resembles that of the annealed film directly formed by spin casting. We also obtained surface patterns similar to Figure 2c by letting room temperature flow-coated films order after a period of ~10 months under ambient laboratory conditions, which was apparently long enough to effectively remove a significant amount of residual solvent. This indicates that the amount of residual solvent in the film *as it orders* dictates the BCP ordering pattern (see later).

While BCP cylinders in a perpendicular orientation are often desirable in applications, this morphology is often difficult to form without making modifications of the substrate surface chemistry.[14] However, the presence of residual solvent in our flow-coated films allows us to robustly create BCP films having a perpendicular cylinder orientation over a wide T range at the film surface. There are evident practical advantages of having residual solvent in the film (especially in thicker films where substrate-induced ordering is difficult) from the standpoint of a materials fabrication strategy.

Neutron Scattering Verification of Basic Model of BCP Film Structure. The PS and PMMA blocks exhibit asymmetric affinities for the solid substrate and the air interface, which is a source of "frustration" in the ordering process. In practice, the PMMA block preferentially segregates to the solid substrate,[1,13] while PMMA and PS have nearly an equal affinity for the polymer–air interface (PS should be slightly more favorable in the T range of our measurements).[16,26] While the presence of residual solvent in the film can be expected to shift these interactions somewhat,[24] the qualitative tendency of these polymers to segregate toward these surfaces should be largely preserved.

Our initial intent in the present work was simply to map out the surface morphology diagram of our BCP films as a function of h_f and T; the residual solvent effect was only discovered when we checked the consistency of our flow-coated films observations with those our group made previously on the same BCP films prepared by spin coating.[18] Since the surface patterns suggest a robust tendency of the flow-coated films to exhibit the interesting standing up cylinder configuration

at the film surface, we restrict our attention primarily to samples prepared by flow coating. Before pursuing this development, we use NR to establish the qualitative ordering pattern in the film responsible for the surface patterns.

We next introduce our working model of the BCP film morphology, which we then support by neutron scattering observations. Provided the qualitative polymer segregation tendencies are preserved in the BCP films with residual solvent, we then expect the BCP to organize upon annealing as in the cartoon in Figure 4. Specifically, the selective interaction of PMMA with the solid substrate noted above should induce cylinder alignment parallel to this interface over a length scale ξ_s where this surface-induced orienting effect is operative. The cylinders near the polymer−air interface are only weakly selective for PS, which can be expected to make this boundary more susceptible to perturbation by residual solvent.

In Figure 5, we show representative NR observations on our BCP films. Neutron reflectivity provides detailed information about the average polymer composition profile normal to the plane substrate, which can be used to validate the schematic model in Figure 4. The procedure for determining the BCP film morphology follows a method developed earlier by Karim et al.[27] and a schematic of the best fit composition profile in relation to a schematic BCP geometry is shown as an inset in the lower left of Figure 5. (This inset is meant to be an aid in interpreting the real fitted NR profile data.) More extensive neutron scattering observations about residual solvent-induced orientation transition in block copolymer films will be reported in a separate publication, but here we include some basic data confirming our assignment of the BCP geometry in Figure 4 that is important for our discussion below. For semideuterated block-copolymers, the scattering length density (SLD) can be used as a measure of the relative polymer composition. In particular, the casting solvent (toluene) is not deuterated in these measurements and the film has been subject to a long thermal annealing process (15 h) at 165 °C so that the residual solvent has largely been removed.

Note that the perpendicular cylinder layer (flat region of the SLD curve near the air interface) extends about 37 nm into the film. Near the solid substrate (within about 40 nm of the solid substrate), the cylinders are oriented parallel to substrate, and the oscillatory SLD curve then reflects the periodic packing of these structures parallel to the plane substrate. The center of the film evidently exhibits a mixed morphology (see Figure 4), as found in the surface morphology when varying h_f, that cannot be assigned purely to a standing up or laying down cylinder morphology.

We can obtained further information about the internal ordering in the nanostructured films by using a relatively new neutron scattering method, rotational
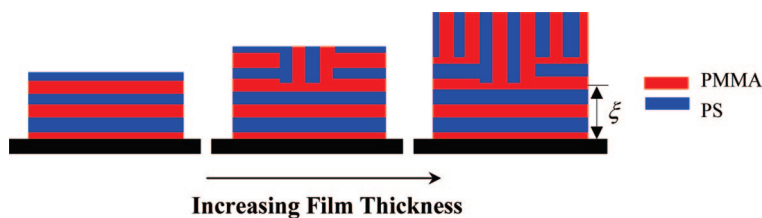

Figure 4. Schematic cross-sectional representation of an annealed PS-*b*-PMMA BCP film.

small angle neutron scattering (RSANS). In this method, the scattering intensity is accumulated as a function of sample rotation angle.

The RSANS intensity was accumulated as a function of sample rotation angle. By reorienting the sample, the scattering pattern becomes sensitive to order along different planes through the scattering volume. Figure 6 shows the reconstructed reciprocal-space scattering intensity maps in a sample coordinate system (the z-axis points along the film normal, and the samples lies in the x−y plane). Figure 6 shows the scattering for a sample that exhibits the vertical texture by AFM. The scattering map shows a weak peak at $Q_x = 0.19$ nm^{-1}, which arises from the cylinder period. While the BCP morphology within BCP films cannot be determined by AFM, RSANS enables us to determine the BCP orientation within the film. As a reference case, a film in which all the cylinders are oriented randomly normal to the substrate would generate a uniform ring of scattering intensity for $Q = \sqrt{(Q_x + Q_z)} = 0.19$ nm^{-1}. The peaking of the scattering peak at $Q_x = 0.19$ nm^{-1} seen in Figure 6 indicates that the cylinders are instead vertically oriented (within some angular distribution). Moreover, the two intense vertical peaks at $Q_x = 0.16$ nm^{-1} are consistent with the presence of some cylinders in a horizontal, hexagonally packed cylindrical morphology. Thus, the neutron reflectivity and RSANS data in Figures 5 and 6 are both consistent with the schematic BCP film morphology indicated in Figure 4 and indirectly in-
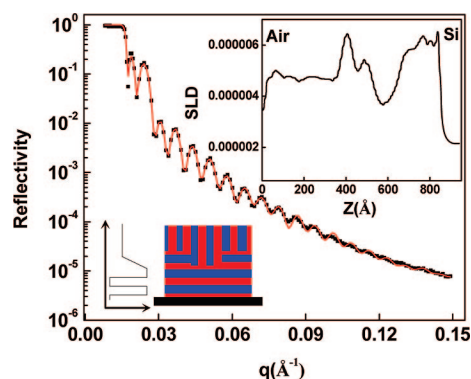

Figure 5. Neutron reflectivity measurements on a flow-coated and annealed dPS-*b*-PMMA film. The deuteration of the PS allows for a determination of the mass distribution of the two polymer species as a function of film height (*z*) and the corresponding fitted scattering length density (SLD) profile is shown as an inset (high SLD corresponds to high dPS concentration).
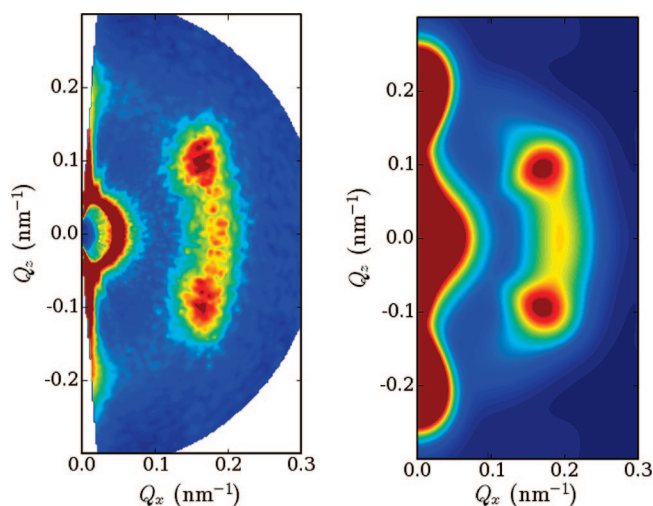
Figure 6. Rotational small-angle neutron scattering (SANS) data (left) of a 141 nm flow-coated and annealed dPS-*b*-PMMA film. The reciprocal-space maps were reconstructed by accumulating SANS data as a function of sample rotation angle. The casting solvent (toluene) is not deuterated in these measurements and the film has been subject to a long thermal annealing process (15 h) at 147 °C. The corresponding fit to the data (right) allows a quantitative estimation of the relative contributions of parallel and perpendicular cylinder orientation populations.

ferred from AFM measurements of the film surface morphology.

The spatial extent or surface correlation length ξ_s (see Figure 4) of the boundary-induced ordering can be expected to vary with T, and the substrate surface energy and the film structure should change for thicknesses greater or less than this scale. This type of surface-induced ordering and the corresponding correlation length has been extensively investigated in the case of diblock copolymers.[6] In relatively thick films, the substrate-oriented interfacial layer should be separated from the region far above where ordering should be dominated by the polymer−air interface where the

interfacial morphologies may coexist in the layer. By varying the film thickness h_f relative to ξ_s, we then expect to see a film morphology variation, provided the ordering at the polymer−air interface is different from that at the polymer−substrate interaction. Toluene is a good solvent for both PS and PMMA and the segregation of toluene to the polymer−air interface is then expected to weaken the already weak preference for polystyrene to segregate to the polymer−air interface in our flow-coated films.[24] The resulting "neutral" boundary condition at this interface would then lead to a robust tendency for the BCP cylinders to orient normal to the polymer−air interface. This effect is apparent for our flow-coated films, but the tendency toward a perpendicular cylinder orientation is not as strong as for spin-cast films where the NR measurements above show that the toluene concentration at the polymer−air interface is small.

We also observe that ξ_s is T dependent. To quantify the T dependence of this basic interfacial scale, the BCP samples were annealed on a silicon oxide wafer for 15 h at T ranging from 129 to 178 °C. Figure 7 shows AFM phase images of PS-*b*-PMMA block copolymers with $h_f = 86$ nm, after annealing for 15 h. A 2D fast-Fourier-transform (FFT) of Figure 7b is indicated in Figure 7h.

Above 155 °C, cylinders oriented parallel to the substrate surface are observed and, below 155 °C, perpendicular cylinders form near the air surface so that a transition in the surface pattern morphology can indeed be induced by varying T. Notably, the cylinders become oriented parallel to the substrate, as in Figure 7e, after a rather short annealing time. Specifically, we checked this effect on films annealed for only 30 min and found this structure to be well established at this time. To check for a further evolution of structure at later times,
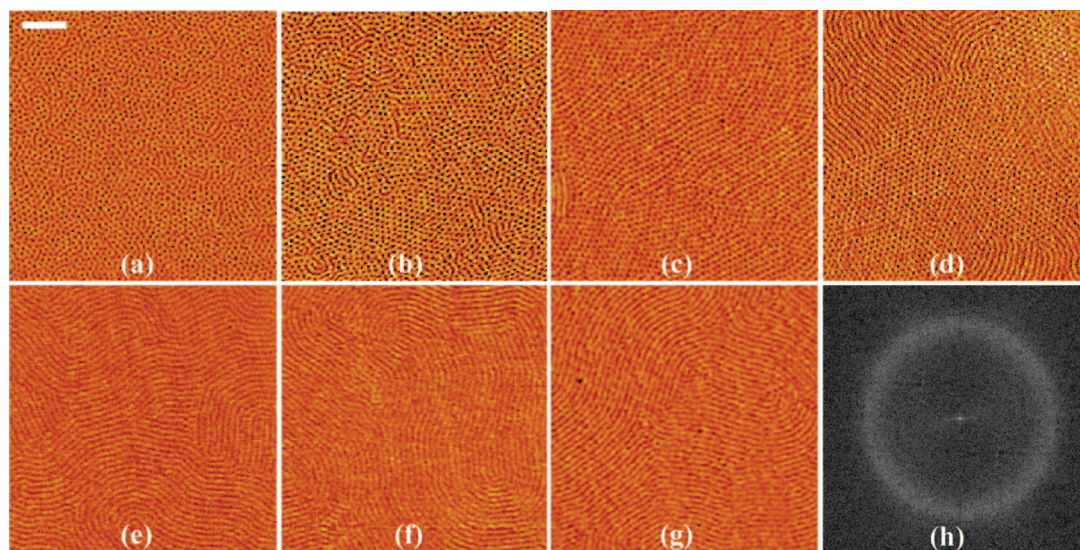

Figure 7. AFM phase images of PS-*b*-PMMA block copolymers with $h_f = 86$ nm after annealing for 15 h at different T: (a) 129, (b) 138, (c) 147, (d) 155, (e) 164, (f) 173 and (g) 178 °C; (h) FFT of panel b. The scale bar in panel a corresponds to 200 nm and also applies to panels b−g.
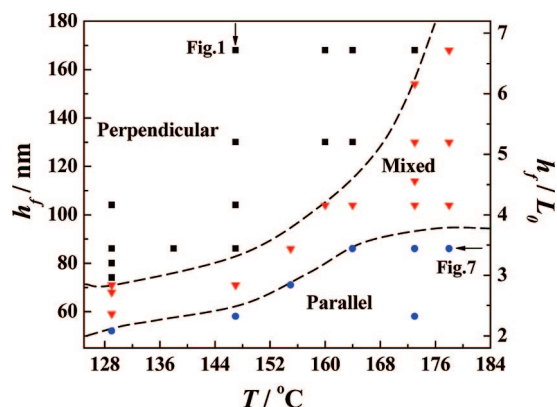
Figure 8. Surface morphology diagram of PS-*b*-PMMA block copolymer films on oxide−silicon substrate. The squares, triangles, and circles represent perpendicular cylinders, mixed-orientation cylinders, and parallel cylinders, respectively. Perpendicular and parallel arrows point to data points corresponding to images in Figures 1 and 7, respectively. The dotted lines are only a guide to the eyes. The standard relative uncertainty associated with the film thickness measurement is ±1 nm.

we examined these films after 3, 6, 15, and 22 h (images not shown) to determine if any evolution occurred at still longer times. No significant evolution of the surface pattern morphology was observed for these films over this extended time range, and indeed we saw no significant evolution in any of our film samples at the other thermodynamic conditions investigated. In certain cases, we followed the evolution for several days to improve our confidence that there was not appreciable further evolution on reasonable timescales.

We also found coexisting cylinder morphologies oriented both parallel and perpendicular to the substrate after annealing films having a thickness $h_f = 86$ nm at 155 °C. These observations show that that the scale ξ_s is on the order of several bulk cylinder period distances and depends on T (see below). As T is gradually decreased, we consistently see a surface pattern transformation from long continuous stripe patterns to short discontinuous stripe patterns characteristic of mixed cylinder orientations, and eventually there is a transition at lower T to perpendicular cylinders.

Construction and Interpretation of BCP Surface Morphology Diagram. Continuing our measurements as a function of T and h_f allows us to construct a "surface morphology diagram" indicating how the surface morphology depends on ordering or "annealing temperature" T and film thickness h_f and the results of this systematic mapping are shown in Figure 8. This figure summarizes our observations (lines are only rough indications of the morphology transition lines) as a function of h_f, h_f/L_0, and T. The repeat period of the block copolymer L_0 is obtained by taking a fast-Fourier-transform (FFT) of the AFM image of a BCP surface pattern in a perpendicular cylinder orientation and a representative FFT is shown in Figure 7h. By taking a circular average of the intensity of the ring pattern in this figure, we obtain the average characteristic wave vector, $\mathbf{q}^*$, where the FFT intensity peaks. The repeat period of the block copolymer is then evaluated from the relation, $L_0 = 2\pi/\mathbf{q}^*$, which leads to the determination, $L_0 = 26$ nm.

Figure 8 indicates that the upper morphology transition line $h_{fu}(T)$ (upper curve in Figure 8), separating the perpendicular and mixed-orientation surface patterns monotonically increases with T. We note that previous studies have established the existence of a corresponding surface correlation length in polymer blends, associated with a boundary-induced surface segregation of one of the blend components, and experiments have also indicated that this scale increases with T as the blend critical temperature for phase separation is approached from below.[28] While a broadening of the surface-induced ordering length in the BCP film is likewise expected upon increasing temperature toward the disordered regime, thin BCP films, such as in our measurements, are normally considered to be in the strong segregation regime so that any temperature-induced change in surface segregation in BCP films might be expected to be weak. However, the presence of residual solvent in our flow-coated films makes this conclusion uncertain and, indeed, previous measurements on flow-coated lamellae-forming PS-*b*-PMMA block copolymer films provided evidence for the proximity of an order−disorder transition temperature in BCP films having comparable film thicknesses to those of the present work.[7] It would certainly be helpful in interpreting this kind of data to have measurements on the effect of residual solvent on the order−disorder transition temperature. Little is known about the location of the order−disorder transition in thin block copolymer films, and the presence of residual solvent in these films adds to this uncertainty. Given this situation, it is difficult to make a definitive interpretation of the surface-induced ordering scale (ξ_s) that is apparent in Figure 8. Below, we discuss evidence that the physics of glass-formation also influences this "lower surface morphology transition line", $h_{fl}(T)$.

The polymer-substrate interaction is often taken as the deciding factor in the orientation of BCP materials in thin films. As mentioned before, the selective nature of the PMMA with the substrate qualitatively explains the parallel orientation in Figure 8. While the presence of the residual solvent must modify the strength of this selective interaction, there is no qualitative change in this surface-induced ordering. Figure 3 shows that only a relatively small amount of solvent is retained near the polymer−air interface, but even a small amount of solvent is probably sufficient to modify the location of this subtle compensation condition. Our observations clearly suggest that the residual solvent within the film is causing the neutral boundary condition to occur at a lower T than one might expect from the pure BCP system. It is this effect that apparently favors the cylinder morphology in our flow-coated BCP films. Note that it is

the presence of residual solvent within the BCP film *as it orders* that is significant for the film morphology; once ordering has occurred and the solvent has been driven off, the high energetic barrier to pass to another morphology and reduction of mobility due to the loss of solvent cause the BCP to become trapped in a metastable state. Our observation that the BCP exhibit a laying down cylinder configuration in spin-cast annealed films under conditions where the flow-coated annealed films give rise to a standing-up cylinder morphology indicates that the upper morphology transition line $h_{fu}(T)$ is not determined by equilibrium thermodynamics alone.

Figure 8 shows another trend that is difficult to rationalize in terms of thermodynamic arguments. Notice that $h_{fl}(T)$ plateaus near 170 °C. This "knee-like" transition curve feature is reminiscent of the saturation effect observed in the wetting−dewetting transition lines of PS films,[29,30] where the "knee temperature" T_{knee} (defining where the saturation effect initiates) was found to track the glass transition temperature T_g for a range of polymer molecular masses from $M = 1800$ to $M = 35000$. In particular, T_{knee}/T_g ratio (ratio in K) was found to equal 1.13 ± 0.03,[29,30] suggesting that glass transition has a direct influence on the surface energy properties of thin polymer films. T_g values of high molecular mass PS and PMMA are comparable (*i.e.*, $T_g \approx 100$ °C) so that the ratio of the saturation temperature (~170 °C) to T_g in Figure 8 is about 1.2. Evidently, the crossover temperature in Figure 8 is comparable to the crossover temperature ($T_c \approx 1.2 T_g$) for glass formation, where the heterogeneity of glass transition starts to become appreciable.[9] Simulations based on self-consistent field theory with local mobility fluctuations suggests that the dynamical heterogeneity of glass formation may indeed influence the block copolymer morphology[9] and conventional crystal growth.[31−34] The knee in the lower transition line in Figure 8 supports the suggestion above that that the BCP film is becoming trapped in a low energy nonequilibrium state in the course of ordering and drying.

CONCLUSIONS

There has been tremendous interest recently in exploiting the molecularly tunable dimensions and morphology of the ordered states of block copolymer materials to create templates and nanoscale interconnect patterns for diverse nanotechnology applications. However, the control of the structure of these materials involves many challenges relating to the perturbation of the thermodynamics of block copolymer ordering in thin films. We thus decided to explore how film thickness and the ordering annealing temperature, the most basic processing variables, influenced the block copolymer surface morphology, the interface of greatest interest from the standpoint of using these materials as nanotemplates. We mapped out two morphology tran-

sition lines [$h_{fu}(T)$, $h_{fl}(T)$] separating the high and low temperature ordering regimes where the surface patterns suggest that the block copolymer cylinders are predominantly standing up and laying down, respectively, from an intermediate regime where these morphologies are strongly mixed. Our initial goal was to develop a working tool to aid technologists in identifying processing conditions allowing the reproducible fabrication of desired block copolymer morphologies for a given application. However, it became apparent from comparing our results on flow-coated films to our earlier work employing spin casting[18] that the method of film preparation is actually important in determining the morphology of solution cast and annealed films. Further measurements were then required to understand why the mode of film casting (i.e., flow-coating versus spin-casting) can yield dramatically different surface morphologies upon ordering starting from the *same* polymer block copolymer solution, film casting at the same temperature, followed by ordering the amorphous block copolymer film of the same thickness and at the same temperature above the glass transition.

Suspecting that residual solvent effects were at play in these films on the basis of our former work on studying crystallization in polymer blend films,[35] we performed neutron reflectivity measurements on both spin-cast and flow-coated films and found that the films vitrify upon casting at room temperature with an appreciable amount of the casting solvent, 12% to 16% by volume, respectively. In hindsight, the origin of this large of amount of solvent in these films is obvious. This is just the solvent composition in which the solution glass transition temperature of the vitrified drying film and room temperature are the same. Evidently, the amount of residual solvent can be controlled by adjusting the temperature at which the film is cast, and the amount remaining in cast glassy films at room temperature is normally quite large.

The presence of residual solvent in these solution-cast BCP films is an intrinsic problem since raising the temperature above the glass transition to remove it causes the BCP to order while the solvent is still in the film. This is the origin of the nonequilibrium morphology variations that we observe, the variations being associated with the distribution of the solvent in the cast film which depends on the method of film formation. We also learn from this study that it is the composition in the film while it is ordering that plays a predominant role in determining the ultimate film morphology in these glassy polymer films.

The influence of the residual solvent in solvent-cast polymer films is not entirely negative, however. In the case of our flow-coated films, where neutron reflectivity measurements indicate that the polymer−air surface of the flow-coated film is locally enriched with toluene relative to a spin-cast film where there is virtually

no toluene at this interface, we obtain a robust tendency of the cast films to form surface patterns consistent with the technologically interesting standing up morphology. (It is generally hard to obtain this morphology in the spin-cast films and great efforts are made to achieve this by adjusting the boundary condition on the solid substrate to have an unselective affinity for both the polymer blocks.[36]) Given the practical importance of this result and the obvious need to exert better control on the morphology of these block copolymer films, we performed neutron reflectivity and employed a new neutron scattering method for BCP characterization, rotational small angle neutron scattering (RSANS), to confirm our tentative assignment of the interior film morphology based on our AFM measurements. These measurements allowed us to confirm our working model of the block copolymer film structure, and we then returned to the general problem of understanding the meaning of the trends we observed in our surface morphology diagram.

Our observations collectively suggest the following picture of the block copolymer ordering process. The selective interaction of one of the block copolymers (PMMA) for the solid substrate causes the BCP cylinders near this boundary to orient parallel along the substrate. This substrate-induced ordering is limited to a correlation length (ξ_s) on the order of a few block copolymer domain spacings, and for films thicker than this

characteristic scale we find a mixed morphology, reflecting the competitive effect of ordering induced by the solid and air interfaces. While it is unclear whether this is an equilibrium or metastable film morphology, it reproducibly occurs in our flow-coated films and the patterns seem to persist indefinitely in time as a practical matter. In still thicker films, the surface patterns mainly reflect the ordering induced by the polymer–air interface, which in our flow-coated films must be influenced by the appreciable amount of the unselective good solvent, toluene, as noted before. This solvent surface segregation apparently explains the observation of a robust tendency for block copolymer cylinder formation in a perpendicular orientation in our thick film regime [above $h_{fu}(T)$ in the surface morphology diagram]. The lower morphology transition line $h_{fl}(T)$ resembles previous observations of the wetting–dewetting transition line in PS polymer films, where there was likewise evidence that the wetting–dewetting transition line was influenced by the physics of glass formation. This formation of standing up cylinders in flow-coated films, and the prospect that the morphology of block copolymer films can be controlled to some degree through the choice of solvent and casting temperature, is a matter of some practical importance in applications where the perpendicularly oriented cylinder morphology is sought as a template for nanomanufacturing.

EXPERIMENTAL DETAILS

Preparation of BCP Thin Films. PS-*b*-PMMA with a total relative molecular mass of 47.7 kg/mol and a mass fraction of PS of 0.74 was purchased from Polymer Source, Inc.[37] dPS-*b*-PMMA with a total relative molecular mass of 77.5 kg/mol and a mass fraction of PS of 0.74 was synthesized in Oak Ridge National Laboratory. Deuterated toluene was purchased from Sigma-Aldrich Inc. PS-*b*-PMMA and dPS-*b*-PMMA films were prepared *via* spin coating and flow coating[38] from a 4% by mass block copolymer solution in toluene onto the plasma-treated Si wafer. The film thickness was characterized with UV–vis interferometry (0.5 mm diameter beam, with standard uncertainty of ±1 at 500 nm film thickness). The samples were placed in a vacuum oven to anneal at different *T* for 15 h. For the residual solvent measurement, PS-*b*-PMMA films were prepared *via* spin coating and flow coating[38] from 4% by mass block copolymer in deuterated toluene onto the plasma treated Si wafer. A typical procedure for generating a block copolymer film *via* flow coating is outlined as follows. The substrate is affixed to the translation stage. A knife blade is mounted on the tip-tilt-rotation stage. The blade is positioned at a fixed angle of 5° in our system and brought down into contact with the substrate. At this point, the blade tilt is adjusted to bring the blade level with the surface of the substrate. The blade is then elevated to a given height above the substrate (typically 200 μm), and a bead of polymer solution (typically 50 μL for a 25-mm-wide blade) is syringed along the leading edge of the blade. Since the blade height is only a couple hundred μm, capillary forces wick and hold the solution under the blade. Once the solution is placed under the knife blade, the operational commands are sent to the translation stage to initiate the desired motion. As the stage moves, a liquid film remains behind. The liquid film then dries to a solid film whose thickness is determined by the solids concentration in the wet film.

Atomic Force Microscope (AFM). AFM images were obtained in both height and phase modes with an Asylum MPF-3D scanning force microscope in the tapping mode. The tapping mode cantilevers with spring constant ≈ 50 N/m, resonance frequency ranging from 100 to 200 kHz, and the drive frequency with the offset of −5% were used. Both height and phase images were recorded simultaneously during scanning. The minor phase (PMMA cylinders) and major phase (PS matrix) correspond to darker and lighter regions in the AFM image, respectively. To obtain the real space images of AFM to avoid artifacts, the samples with the same annealing conditions were scanned in multiple positions in order to get more images at 2 μm × 2 μm.

Neutron Reflectivity (NR). The NR experiments were conducted at the NIST Center for Neutron Research at the National Institute of Standards and Technology. The NG7 horizontal reflectometer utilized a 4.76 Å collimated neutron beam with a wavelength divergence of 0.18 Å. The angular divergence of the beam was varied through the reflectivity scan and this provided a relative q resolution dq/q of 0.04, where $q = 4\pi \sin(\theta)/\lambda$, and θ is the incident and final angle with respect to the surface of the film. Scans were made over a wavevector magnitude (q) range from 0.05 to 0.13 Å^{-1}. Conversion of the NR spectra to the scattering length density (SLD) and concentration profiles was done using the NRSA software provided by Charlie Laub (University of California, Davis).[20]

Small-Angle Neutron Scattering (SANS). Rotational SANS experiments were conducted using the NG7-SANS instrument at the NIST Center for Neutron Research, using an incident wavelength of 6.0 Å and a wavelength divergence of 0.74 Å. The 2-D images are taken from a series of incidence angles and the measurements are made in transmission. Footprint corrections were applied by normalizing the scattering data using the intensity along the rotation axis (Q_y). Data was fit by extending the model of Ruland and Smarsly[39] to allow for both parallel and perpen-

dicular populations of cylinders, each with an orientational distribution. Instrumental resolution was explicitly included using established methods.[40]

REFERENCES AND NOTES

1. Bates, F. S.; Fredrickson, G. H. Block Copolymer Thermodynamics: Theory and Experiment. *Annu. Rev. Phys. Chem.* **1990**, *41*, 525–557.

2. Wang, Q.; Nealey, P. F.; de Pablo, J. J. Monte Carlo Simulations of Asymmetric Diblock Copolymer Thin Films Confined between Two Homogeneous Surfaces. *Macromolecules* **2001**, *34*, 3458–3470.

3. Rockford, L.; Mochrie, S. G. J.; Russell, T. P. Propagation of Nanopatterned Substrate Templated Ordering of Block Copolymers in Thick Films. *Macromolecules* **2001**, *34*, 1487–1492.

4. Park, M.; Harrison, C.; Chaikin, P. M.; Register, R. A.; Adamson, D. H. Block Copolymer Lithography: Periodic Arrays of ~10^{11} Holes in 1 Square Centimeter. *Science* **1997**, *276*, 1401–1404.

5. Harrison, C.; Park, M.; Chaikin, P. M.; Register, R. A.; Adamson, D. H. Lithography with a Mask of Block Copolymer Microstructures. *J. Vac. Sci. Technol. B* **1998**, *16*, 544–552.

6. Fredrickson, G. H. Surface Ordering Phenomena in Block Copolymer Melts. *Macromolecules* **1987**, *20*, 2535–2542.

7. Smith, A. P.; Douglas, J. F.; Amis, E. J.; Karim, A. Effect of Temperature on the Morphology and Kinetics of Surface Pattern Formation in Thin Block Copolymer Films. *Langmuir* **2007**, *23*, 12380–12387.

8. Kim, S. H.; Misner, M. J.; Xu, T.; Kimura, M.; Russell, T. P. Highly Oriented and Ordered Arrays from Block Copolymers *via* Solvent Evaporation. *Adv. Mater.* **2004**, *16*, 226–231.

9. Bosse, A. W.; Douglas, J. F.; Berry, B. C.; Jones, R. L.; Karim, A. Block Copolymer Ordering with a Spatiotemporally Heterogeneous Mobility. *Phys. Rev. Lett.* **2007**, *99*, 216101-1–216101-4.

10. Suh, K. Y.; Kim, Y. S.; Lee, H. H. Parallel and Vertical Morphologies in Block Copolymers of Cylindrical Domain. *J. Chem. Phys.* **1998**, *108*, 1253–1256.

11. Horvat, A.; Knoll, A.; Krausch, G.; Tsarkova, L.; Lyakhova, K. S.; Sevink, G. J. A.; Zvelindovsky, A. V.; Magerle, R. Time Evolution of Surface Relief Structures in Thin Block Copolymer Films. *Macromolecules* **2007**, *40*, 6930–6939.

12. Thurn-Albrecht, T.; Steiner, R.; DeRouchey, J.; Stafford, C. M.; Huang, E.; Bal, M.; Tuominen, M.; Hawker, C. J.; Russell, T. P. Nanoscopic Templates from Oriented Block Copolymer Films. *Adv. Mater.* **2000**, *12*, 787–791.

13. Coulon, G.; Russell, T. P.; Green, P. F.; Deline, V. R. Surface-Induced Orientation of Symmetric, Diblock Copolymers: A Secondary Ion Mass-Spectrometry Study. *Macromolecules* **1989**, *22*, 2581–2589.

14. Huang, E.; Pruzinsky, S.; Russell, T. P.; Mays, J.; Hawker, C. J. Neutrality Conditions for Block Copolymer Systems on Random Copolymer Brush Surfaces. *Macromolecules* **1999**, *32*, 5299–5303.

15. Orso, K. A.; Green, P. F. Phase Behavior of Thin Film Blends of Block Copolymers and Homopolymers: Changes in Domain Dimensions. *Macromolecules* **1999**, *32*, 1087–1092.

16. Morkved, T. L.; Lopes, W. A.; Hahm, J.; Sibener, S. J.; Jaeger, H. M. Silicon Nitride Membrane Substrates for the Investigation of Local Structure in Polymer Thin Films. *Polymer* **1998**, *39*, 3871–3875.

17. Ham, S.; Shin, C.; Kim, E.; Ryu, D. Y.; Jeong, U.; Russell, T. P.; Hawker, C. J. Microdomain Orientation of PS-*B*-PMMA by Controlled Interfacial Interactions. *Macromolecules* **2008**, *41*, 6431–6437.

18. Berry, B. C.; Bosse, A. W.; Douglas, J. F.; Jones, R. L.; Karim, A. Orientational Order in Block Copolymer Films Zone Annealed below the Order-Disorder Transition Temperature. *Nano Lett.* **2007**, *7*, 2789–2794.

19. Lin, Z.; Kim, D. H.; Wu, X.; Boosahda, L.; Stone, D.; LaRose, J.; Russell, T. P. a Rapid Route to Arrays of Nanostructures in Thin Films. *Adv. Mater.* **2002**, *14*, 1373–1376.

20. Laub, C. F.; Kuhl, T. L. Fitting a Free-Form Scattering Length Density Profile to Reflectivity Data Using Temperature-Proportional Quenching. *J. Chem. Phys.* **2006**, *125*, 244702-1–244702-8.

21. Tsige, M.; Grest, G. S. Solvent Evaporation and Interdiffusion in Polymer Films. *J. Phys. Condens. Matter* **2005**, *17*, S4119–S4132.

22. Croll, S. G. The Origin of Residual Internal Stress in Solvent-Cast Thermoplastic Coatings. *J. Appl. Polym. Sci.* **1979**, *23*, 847–858.

23. Ferry, J. D. *Viscoelastic Properties of Polymers*, 3rd ed.; Wiley: New York, 1980; pp 486–544.

24. Garcia-Turiel, J.; Jerome, B. Solvent Retention in Thin Polymer Films Studied by Gas Chromatography. *Colloid Polym. Sci.* **2007**, *285*, 1617–1623.

25. Soles, C. L.; Douglas, J. F.; Wu, W. L. Dynamics of Thin Polymer Films: Recent Insights from Incoherent Neutron Scattering. *J. Polym. Sci., Part B* **2004**, *42*, 3218–3234.

26. Sivaniah, E.; Hayashi, Y; Matsubara, S.; Kiyono, S.; Hashimoto, T. Symmetric Diblock Copolymer Thin Films on Rough Substrates. Kinetics and Structure Formation in Pure Block Copolymer Thin Films. *Macromolecules* **2005**, *38*, 1837–1849.

27. Karim, A.; Singh, N.; Sikka, M.; Bates, F. S.; Dozier, W. D.; Felcher, G. P. Ordering in Aymmetric Poly(ethylene-propylene)−Poly(ethylene) Diblock Copolymer Thin Films. *J. Chem. Phys.* **1994**, *100*, 1620–1629.

28. Grüll, H.; Sung, L.; Karim, A.; Douglas, J. F.; Satija, S. K.; Hayashi, M.; Jinnai, H.; Hashimoto, T.; Han, C. C. Finite-Size Effects on Surface Segregation in Polymer Blend Films above and below the Critical Point of Phase Separation. *Europhys. Lett.* **2004**, *65*, 671–677.

29. Ashley, K. M.; Raghavan, D.; Douglas, J. F.; Karim, A. Wetting−Dewetting Transition Line in Thin Polymer Films. *Langmuir* **2005**, *21*, 9518–9523.

30. The temperature ratios were inadvertently discussed in term of their ratios in °C in ref 26 rather than in K.

31. Gránásy, L.; Pusztai, T.; Warren, J. A.; Douglas, J. F.; Börzsönyi, T.; Ferreiro, V. Growth of 'Dizzy Dendrites' in a Random Field of Foreign Particles. *Nat. Mater.* **2003**, *2*, 92–96.

32. Gránásy, L.; Pusztai, T.; Börzsönyi, T.; Warren, J. A.; Douglas, J. F. A General Mechanism of Polycrystalline Growth. *Nat. Mater.* **2004**, *3*, 645–650.

33. See ref 9 for an analogous discussion of the influence of dynamic heterogeneity of glass-formation on BCP ordering.

34. Gránásy, L.; Pusztai, T.; Tegze, G.; Warren, J. A.; Douglas, J. F. Growth and Form of Spherulites. *Phys. Rev. E* **2005**, *72*, 011605-1–011605-14.

35. Ferreiro, V.; Douglas, J. F.; Warren, J.; Karim, A. Growth Pulsations in Symmetric Dendritic Crystallization in Thin Polymer Blend Films. *Phys. Rev. E* **2002**, *65*, 051606-1–051606-16.

36. Mansky, P.; Liu, Y.; Huang, E.; Russell, T. P.; Hawker, C. J. Controlling Polymer-Surface Interactions With Random Copolymer Brushes. *Science* **1997**, *275*, 1458–1460.

37. Certain equipment, instruments or materials are identified in this paper to adequately specify the experimental details. Such identification does not imply

recommendation by the NIST, nor does it imply the materials are necessarily the best available for the purpose.

38. Stafford, C. M.; Roskov, K. E.; Epps, T. H.; Fasolka, M. J. Generating Thickness Gradients of Thin Polymer Films *via* Flow Coating. *Rev. Sci. Instrum.* **2006**, *77*, 023908-1– 023908-7.

39. Ruland, W.; Smarsly, B. SAXS of Self-Assembled Nanocomposite Films with Oriented Two-Dimensional Cylinder Arrays: An Advanced Method of Evaluation. *J. Appl. Crystallogr.* **2005**, *38*, 78–86.

40. Pedersen, J. S.; Posselt, D.; Mortensen, K. Analytical Treatment of the Resolution Function for Small-Angle Scattering. *J. Appl. Crystallogr.* **1990**, *23*, 321–333.

ARTICLE